

Observed Damping of Barotropic Seiches through Baroclinic Wave Drag in the Gullmar Fjord

RICHARD PARSMAR AND ANDERS STIGEBRANDT

Department of Oceanography, University of Göteborg, Göteborg, Sweden

(Manuscript received 7 August 1995, in final form 11 February 1996)

ABSTRACT

Baroclinic wave drag, due to internal wave generation at steep topography, is shown to be a mechanism that effectively subdues barotropic seiches in fjords. A two-layer model for a fjord with a sill at the mouth is applied to the Gullmar Fjord, Sweden. The damping of the fundamental seiche mode observed from sea level records is well predicted by the model. This includes the observed seasonal variation in damping due to the corresponding variation in vertical stratification. It is shown that ordinary bottom friction should contribute less than 1% to the damping in this fjord.

Simultaneous current records from different depths, obtained on the slope of the sill in the fjord, are analyzed. Spectra of all records show a significant energy peak at the seiche frequency. The vertical variation of the phase of the current at this frequency shows that the motion is essentially baroclinic.

1. Introduction

A long barotropic natural mode of oscillation with a node at the fjord mouth, a seiche, is a prominent feature in sea level records from Bornö Hydrographical Station in the Gullmar Fjord, Sweden (Fig. 1). The fundamental mode, with a period of approximately 1 h 56 min, totally dominates over higher modes. The seiche occurs frequently with maximum amplitudes in the range 2–15 cm. The seiche was analyzed and discussed by Zeilon (1913) who also noted that a vertical oscillation with the period of the barotropic seiche was evident in the halocline. The latter was recorded at Bornö by a so-called boundary gauge (halocline rider) constructed in 1910 by Otto Pettersson; see Kullenberg (1932). Zeilon claimed that these internal waves are topographically related to the surface seiche in the same way as internal tidal waves are related to the surface tide, a relationship he earlier investigated in Zeilon (1912). He thought that the baroclinic waves with the period of the barotropic seiche consist of a system of progressive waves. However, the energy transfer from the barotropic seiche to baroclinic waves and the damping of the surface seiche, the themes of the present paper, were not discussed by Zeilon (1913).

Provided that the topography of a fjord is not very

complicated, the strongest currents due to the fundamental seiche should occur at the mouth. If the vertical cross-sectional area of the fjord mouth is reduced by the presence of a sill, this will further enhance the current there. Thus, strong currents across steep topography are mainly found at the mouth of sill fjords. Generation of internal waves by oscillating barotropic currents across steep topography is a well-known phenomenon described in several papers, for example, Zeilon (1912), Proudman (1953), Rattray (1960), Stigebrandt (1976, 1980), Baines (1982), de Young and Pond (1989), and Sjöberg and Stigebrandt (1992).

This paper is devoted to processes that remove energy from barotropic seiches in fjords. In particular, we consider energy transfer from barotropic seiches to progressive internal waves taking place at fjord sills. An expression for the damping of a seiche by such baroclinic wave drag has been derived earlier and applied to the inner Oslo Fjord (Stigebrandt 1976). It was concluded that a barotropic seiche in that fjord should be so strongly damped that it hardly would be detectable. This was confirmed by the apparent absence in sea level records of barotropic seiches with nodes at the mouth. To our knowledge, damping of seiches in fjords has not been studied in other papers.

A slightly modified version of the model in Stigebrandt (1976) is used to estimate the damping of the seiche in the Gullmar Fjord by baroclinic wave drag. The modification essentially includes internal wave drag also occurring at the seaward side of the sill. The theoretical damping will be compared with the damping of the seiche as observed from a one-year-long sea level record. We also analyze current meter data from

Corresponding author address: Dr. Richard Parsmar, Department of Oceanography, Earth Science Center, University of Göteborg, S-413 81 Göteborg, Sweden.
E-mail: ripa@oce.gu.se

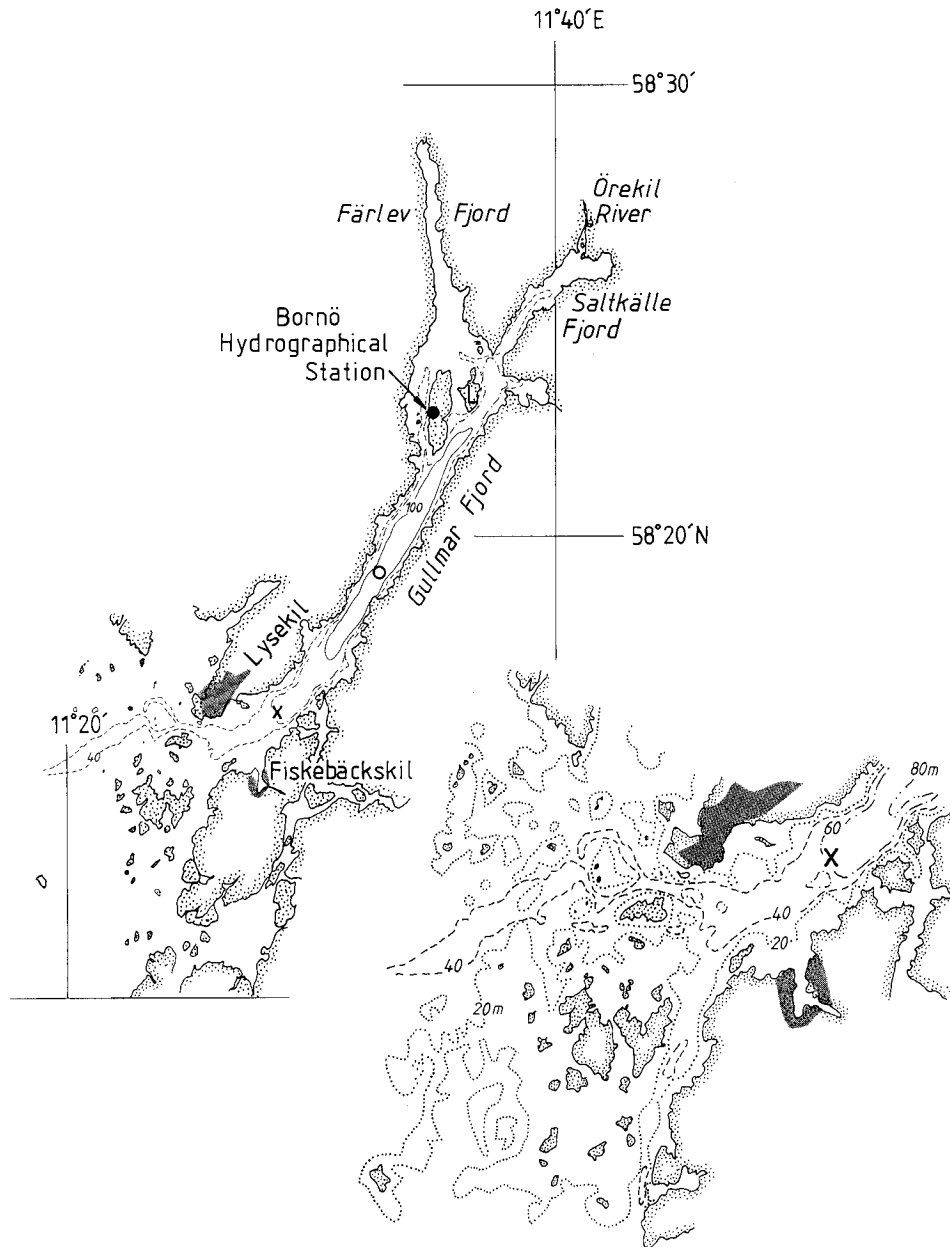


FIG. 1. Map over Gullmar Fjord. The current meter mooring is marked by (X), the position of the measurements of salinity and temperature is marked with (○), and the Bornö hydrographical station is marked by (●).

three depths located just inside the mouth to demonstrate the presence of internal waves with the frequency of the seiche. Contributions to the damping by bottom friction will be discussed. The paper is concluded by a short discussion of the damping of higher seiche modes and the process of baroclinic wave drag as an efficient low-pass filter. The energy contribution by the internal waves generated by the seiche to turbulence and mixing in the basin water of the fjord is also briefly discussed.

2. Theory

In a rectangular fjord of constant width B , the energy of the fundamental barotropic seiche is E . If the fjord has a sill at its mouth and is vertically stratified, the seiche loses energy through baroclinic wave drag at the sill. Following Stigebrandt (1976), but with the modification that internal waves are allowed to be generated also on the seaward side of the sill, the seiche loses energy to progressive baroclinic waves radiating away

from the sill. The rate of change of seiche energy due to this loss then is

$$\frac{dE}{dt} = -(\epsilon_i + \epsilon_o), \quad (1)$$

where ϵ_i (ϵ_o) is the rate of energy transfer from the barotropic seiche to baroclinic waves inside (outside) the sill.

For a continuous vertical stratification the distribution of internal wave energy among vertical modes depends mainly on the relative height of the sill (Stigebrandt 1980) and the form of the vertical density profile (Sjöberg and Stigebrandt 1992). If the sill height is about half of the height of the water column, which is the case in the Gullmar Fjord, much of the energy should go into the first vertical mode (Stigebrandt 1980). Here we assume that the stratification may be described as two-layered with the mean level of the pycnocline coinciding with the top of the sill. This type of stratification prevails in the Gullmar Fjord, see section 3 below. The situation is then similar to that in Stigebrandt (1976). The energy transfer to progressive baroclinic waves at a sill can be computed as the product of the energy density and group velocity of the waves times the width of the sill. From Stigebrandt (1976) one obtains

$$\epsilon = \frac{\rho_0 u_0^2 A_m}{2H} \frac{dc_i}{c_i}, \quad (2)$$

where ρ_0 is a reference density, u_0 is the amplitude of the oscillating seiche current over the sill, H is the water depth inside (outside) the sill, d is the height over the bottom (which may be different on the two sides of the sill if the H are different), c_i is the phase speed of an interfacial long internal wave (may be different on the two sides of the sill), and A_m is the vertical cross-sectional area of the mouth (above the sill).

The phase speed c_i of long interfacial internal waves in two-layer stratification is

$$c_i = \sqrt{\frac{\Delta\rho(H-d)d}{\rho_0 H g}}, \quad (3)$$

where $\Delta\rho$ is the density difference between the layers and g is the acceleration of gravity (e.g., Gill 1982).

The damping of a barotropic seiche may be described by the damping coefficient C defined by

$$E = E_0 e^{-Ct}, \quad (4)$$

where E_0 is the seiche energy at $t = 0$. This description of the damping is well suited for comparison with observations. The timescale for damping is the inverse of the damping coefficient; C may be written

$$C = -\frac{1}{E} \frac{dE}{dt}. \quad (5)$$

For later comparison with observations we need to derive the theoretical value of C due to baroclinic wave drag, where dE/dt is given by Eq. (1), which is valid

for damping by the combined baroclinic wave drag on both sides of the sill.

In a rectangular fjord of constant depth the sea level η due to a seiche is described by

$$\eta = a_i \sin(kx)\sin(\omega t), \quad (6)$$

where a_i is the amplitude and ω is the frequency. The x axis is directed into the fjord with $x = 0$ at the mouth. The wavenumber is $k = (n + 1/2)\pi L^{-1}$, where $n = 0, 1, 2, \dots$ and L is the length of the fjord. For the fundamental mode n equals 0 and the only node is located in the mouth.

The energy of the seiche in a rectangular fjord of width B may be computed from

$$E = \frac{1}{2} \rho g B \int_0^L \eta^2(x) dx, \quad (7)$$

which is the potential energy at times t equal to $\pi/4, 3\pi/4, \dots$ when the kinetic energy is zero; cf. Eq. (11) below. Using Eq. (6) one finds that

$$E = \frac{1}{4} \rho g a_i^2 A_f. \quad (8)$$

Here $A_f = LB$ is the horizontal surface area of the fjord.

In the following we assume for simplicity that $\epsilon_o = \epsilon_i$; that is, the transfers of energy from the barotropic seiche to baroclinic waves are of equal magnitude inside and outside the sill. This assumption will be discussed later. Using Eqs. (1), (2), (5), and (8) one then obtains

$$C = \frac{4u_0^2 A_m}{g a_i^2 H A_f} \frac{dc_i}{c_i}. \quad (9)$$

The current amplitude $u = u(x)$ of the seiche may be computed from the continuity equation for volume

$$BDu(x) = B \int_x^L w dx, \quad (10)$$

where $w = \partial\eta/\partial t$ is the vertical velocity at the sea surface and the depth D is equal to H in the fjord and $H - d$ at the sill ($x = 0$). Using Eq. (6) one obtains

$$u(x) = \frac{Ba_i\omega}{kBD} \cos(kx)\cos(\omega t). \quad (11)$$

With $BL = A_f$ and $B(H - d) = A_m$ the current amplitude $u_0 = u(0)$ of the seiche at the sill is

$$u_0 = \frac{2a_i\omega A_f}{\pi A_m}. \quad (12)$$

Inserting (12) in (9) yields

$$C = \frac{16d\omega^2 A_f}{\pi^2 g H A_m} \sqrt{\frac{\Delta\rho(H-d)d}{\rho H g}}. \quad (13)$$

This is identical to the expression in Stigebrandt (1976) except for the numerical constant, which here is a factor of about 2 greater since energy transfer to bar-

TABLE 1. Parameter values for application of the model to the Gullmar Fjord. The seiche frequency is an average value.

Fjord area	A_f	51×10^6	(m ²)
Mouth area	A_m	23×10^3	(m ²)
Thickness of the lower layer	d	34	(m)
Thickness of the upper layer	$H - d$	42	(m)
Acceleration due to gravity	g	10	(m s ⁻²)
Seiche angular frequency	ω	9.0×10^{-4}	(s ⁻¹)

oclinic waves is assumed to take place also at the seaward side of the fjord sill. The theoretical damping coefficient C due to baroclinic wave drag given by Eq. (13) will later be compared with the observed damping coefficient of the seiche in Gullmar Fjord. However, we will first discuss energy transfer from the barotropic seiche due to bottom friction.

Ordinary bottom friction may contribute to the damping of barotropic seiches; its magnitude may be estimated in the following way. The stress at the bottom is $\tau = \rho C_D u |u|$, where ρ is the density, C_D the drag coefficient, and u the current velocity of the seiche (first horizontal mode) given by Eq. (11).

The average over a seiche period of the energy transfer to dissipation due to bottom friction in the fjord is given by

$$\sigma = \frac{1}{T} \int_0^T \int_0^l \rho B C_D u^2 |u| dx dt. \quad (14)$$

Using Eqs. (11) and (14) with $BL = A_f$ and $\omega = \pi/2L \sqrt{gD}$ one obtains

$$\sigma = \frac{16\rho C_D A_f a_i^3}{9\pi^2} \left(\frac{g}{D}\right)^{3/2}. \quad (15)$$

This expression may be compared to the energy transfer $\varepsilon_0 + \varepsilon_i = 2\varepsilon_i$ due to baroclinic wave drag at the sill, which may be obtained from Eqs. (2) and (12). One obtains

$$\frac{\sigma}{2\varepsilon_i} = \frac{4C_D H A_m a_i}{9\omega^2 d A_f c_i} \left(\frac{g}{D}\right)^{3/2}. \quad (16)$$

Using $a_i = 0.05$ m, $c_i = 1$ m s⁻¹, $D = 45$ m (the mean depth of the fjord), and $C_D = 0.003$ for the Gullmar Fjord, it follows that $\sigma/2\varepsilon_i \approx 0.008$ (for additional numerical values, see Table 1 above). Thus, the energy flux to the frictional bottom boundary layer is only of the order of 1% of the energy flux to internal waves due to topographic baroclinic wave drag at the sill. For all practical purposes, bottom friction may thus be neglected as a mechanism for seiche damping in this particular fjord.

3. Fjord characteristics

The Gullmar Fjord on the Swedish Skagerrak coast, with length about 30 km and width about 2 km, is oriented approximately in the SW–NE direction (Fig. 1).

The main part of the fjord is straight with steep rocky and rather high shores (~ 100 m). In the inner reaches the fjord is split into two arms: the deep Saltkälle Fjord and the shallow Färlev Fjord. The maximum depth, 118 m, is found about 10 km from the mouth. The mean depth is about 45 m. However, for the two-layer model we take the depth of the upper layer equal to the sill depth (42 m), and the depth of the lower layer is computed as the volume of the sill basin divided by the maximum horizontal surface area of this basin (i.e., at the sill depth). This gives the thickness of the lower layer equal to 34 m (Table 1). The Fjord mouth is wide with irregular topography and islands and the water is quite shallow around the islands. The major connection to the sea is close to Lysekil where the sill depth is about 42 m. As the vertical cross-sectional area of the mouth A_m (Table 1) we have taken the minimum area of the major connection to the sea.

The tide is quite weak in the Skagerrak: The dominating semidiurnal tide has an amplitude of only 0.15–0.20 m. The annual mean freshwater runoff to the fjord is about 25 m³ s⁻¹ (Svansson 1984). Most of this, about 21 m³ s⁻¹, is supplied to the innermost part of the Saltkälle Fjord by the Örekil River. In periods with high runoff, mainly in spring and autumn, there may be a distinct brackish layer occupying the uppermost layer of the fjord.

The density of the coastal water at the Swedish Skagerrak coast varies greatly in response to outflow of low salinity (20–25 psu) water from the Kattegat and time-dependent wind-driven circulation within the Skagerrak (cf. Gustafsson and Stigebrandt 1996). The varying density field outside the Gullmar Fjord forces an intense baroclinic water exchange through the mouth such that the vertical stratification above the sill depth in the fjord is rather similar to the stratification in the coastal water outside the mouth. However, the basin water below the sill level always has high density since the sill traps the densest coastal water occurring at sill depth. Because of this there is almost always a pycnocline at sill level in the fjord.

4. Field data

Sea level recording on paper, that is, a mareograph series, started at Bornö Hydrographical Station around 1911 (Pettersson 1921). Records are reproduced in Zeilon (1913) and Pettersson (1917). We have used recordings from the year 1985 when the sea level was recorded continuously during 341 days.

In August 1974 a rig with three Aanderaa current meters was anchored near the mouth in the Gullmar Fjord (see Fig. 1). For 28 days data were recorded every 10th min. The current meters were placed 4, 30, and 55 m below the sea surface. The bottom depth was 62 m.

The density stratification is computed from measurements of salinity and temperature (see Fig. 1 for the position of the measurements) stored in the hydrograph-

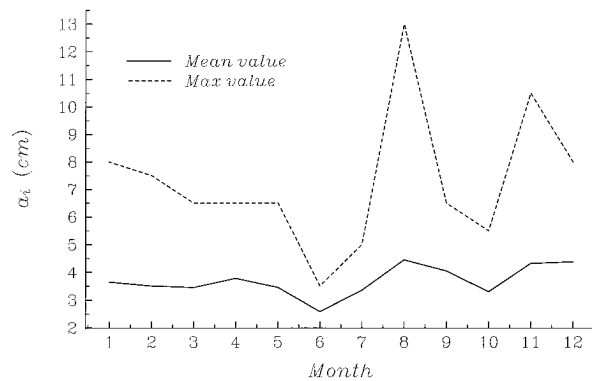


FIG. 2. Monthly mean and maximum seiche amplitude a_i in 1985 as recorded at Bornö.

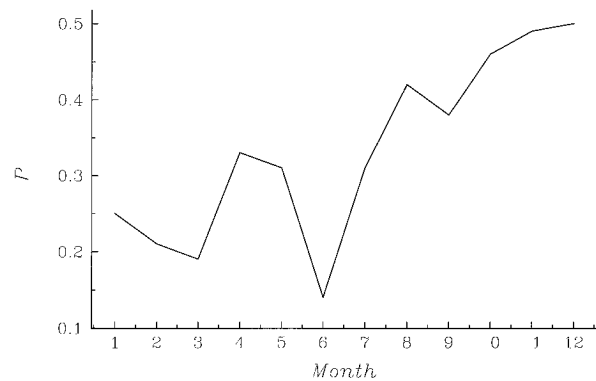


FIG. 3. Monthly probability P of occurrence of the seiche in 1985.

ic database held by the Swedish Meteorological and Hydrological Institute (SMHI). From the year 1985 we found 12 vertical density profiles, one for each month, and for 1974 one profile taken from the 28th of August.

5. Results

First, we determined the period and amplitude of the seiche in 1985. By manual reading of 75 daily sea level records, having a well-developed seiche and evenly distributed over the year, we observed that the seiche period varies in the range $90 < T < 132$ min and that the mean period is 115 min. The variation of the seiche period (also noted by Zeilon 1913) is also confirmed by the spectral analysis of current meter data as discussed later. The reasons for the varying seiche period should probably be found in the topography of the fjord, which permits different modes of oscillation. To explain this is, however, beyond the aim of the present paper.

The seiche amplitude a_i varies from 2 to 13 cm, and from 233 observed amplitudes we obtained a mean value of 3.8 cm for this particular year. In Fig. 2 we show the mean value of the amplitude for each month, and a seasonal variation with maxima in April, August, and November can be seen. The maximum observed amplitude for each month is also plotted in this figure, showing maxima in August and November with values of 13 and 10 cm respectively. Since Bornö is located a distance of about $2L/3$ from the mouth, the seiche amplitudes above should be corrected by multiplication with a factor $1/\sin(\pi/3) \approx 1.15$ in order to obtain a_i more precisely; cf. Eq. (6).

In the model for seiche damping, it is implicitly assumed that the forcing may be neglected in the decay process. This should be true if the seiche is generated in a relatively short period of time. A visual inspection of the sea level records shows that there is no build-up phase with successively increasing amplitude of the seiche, which suggests that the seiche is generated almost instantaneously. This should imply that the seiche is generated by a sudden change (in, maybe, wind stress)

and not by a periodic forcing acting during a longer period of time. The assumption that the forcing may be neglected in the decay process thus seems valid.

Since the sea level has been measured almost continuously, one may investigate the frequency of occurrence of the seiche. The ratio between the number of hours when the seiche can be seen and the total number of hours in the record gives the probability P for the appearance of a seiche. In Fig. 3 we show the probability for each month in 1985. As can be seen, P increases from 0.13 in June to a maximum in December when P equals 0.50. The mean value for the year is $P = 0.33$. The seasonal variation of P is quite similar to the variation of the wind stress; cf. Gustafsson and Stigebrandt (1996). This relationship suggests that the wind is involved in some way in the generation of the seiche. However, mechanisms for seiche generation will not be discussed in the present paper.

For the application of our model, it is necessary to approximate the observed vertical density profile $\rho(z)$ by a two-layer stratification with the "interface" at sill depth and with the densities ρ_1 and ρ_2 in the upper and lower layers respectively. In this approximation we account for the volumetric effects due to the vertical dependence of the horizontal fjord area. The density difference between the two layers, $\Delta\rho = \rho_2 - \rho_1$, is important for the speed of internal waves [Eq. (3)] and by that also for the energy transfer to baroclinic waves [Eq. (2)]. As explained in section 3, there is almost always a pycnocline at sill depth in the Gullmar Fjord. However, the vertical stratification above the sill level varies on the seasonal and shorter timescales (see Fig. 4). The strongest measured stratification during this particular year (1985) occurs in April, August, and October, when the upper layer is relatively fresh. In the lower layer the density varies only slowly during the year. The variation in $\Delta\rho$ is therefore essentially due to the density variation in the upper layer. The annual mean of $\Delta\rho$ based on the monthly measurements in this particular year is 4.3 kg m^{-3} .

Figure 5 shows an example of a barotropic seiche in the sea level record. The amplitude, initially about 13

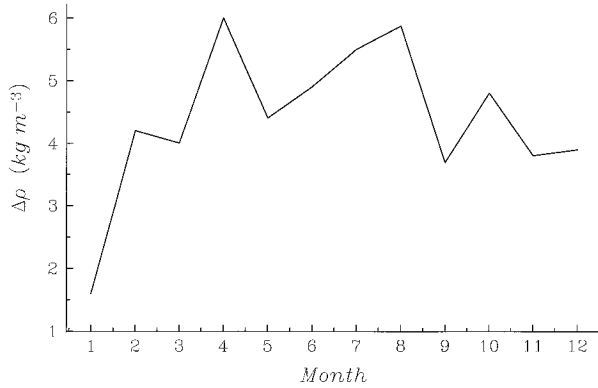


FIG. 4. The observed density difference $\Delta\rho$ between the two layers in 1985.

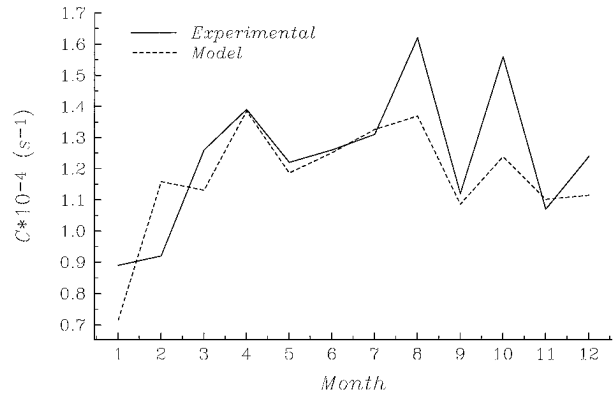


FIG. 6. Model and experimental values of the damping coefficient C monthly means for 1985.

cm, is about 1.5 cm after 8.5 h. Using Eqs. (4) and (8), one obtains an experimental value of C equal to 1.4×10^{-4} . Applying our model, Eq. (13), to Gullmar Fjord with the parameters given in Table 1 and with $\Delta\rho = 5.87 \text{ kg m}^{-3}$ and $\omega = 9.0 \times 10^{-4} \text{ s}^{-1}$, we get $C = 1.36 \times 10^{-4}$. This shows that energy flux to internal waves, in contrast to dissipation due to bottom friction (cf. section 2), is a likely mechanism for the observed damping of the seiche. However, the result, albeit close to the experimental value, is of course sensitive to the choice of parameter values. The most uncertain of these, the density difference $\Delta\rho$ between the two layers, was measured only two days before this seiche event and is therefore considered representative of the stratification during the event.

We compute from the sea level record experimental values of C from 75 occasions in 1985 when the seiche was well developed and find that C varies in the interval $0.43 \times 10^{-4} < C < 2.39 \times 10^{-4}$. From Eq. (13) the damping depends upon ω^2 and $\Delta\rho$. Results show that the seiche in Gullmar Fjord has frequencies in the interval $7.9 \times 10^{-4} < \omega < 11.6 \times 10^{-4}$ and that the

observed stratification in 1985 varies in the interval $1.8 < \Delta\rho < 6.0 \text{ (kg m}^3\text{)}$. As a consequence of the variation in these parameters, the damping described by the model would vary in the interval $0.55 \times 10^{-4} < C < 2.30 \times 10^{-4}$. Thus, the model seems capable of explaining even the observed range of the damping. One might possibly suspect that variations in the seiche period T may be linked to changes in the damping coefficient C . For the 75 occasions the correlation between C and T was, however, found to not be significant ($r = -0.18$).

For each month we compute a mean value of the experimental damping coefficient based on the sea level observations. This value may then be compared with the model prediction. From Fig. 4 we get $\Delta\rho$ for each month and with the parameters given in Table 1 we obtain the result shown in Fig. 6. The experimental values of C are fairly well predicted by the model. Greatest values of C occur in April, August, and October when the stratification is strongest. The experimental values in August and October are a factor of about 1.2 greater than the model values. This corresponds to a density

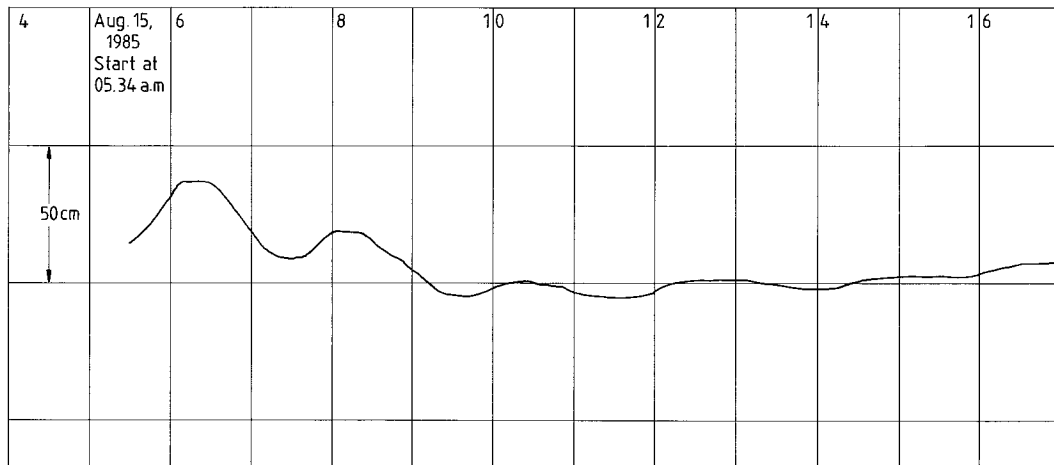


FIG. 5. Sea level record obtained at Bornö 15 August 1985.

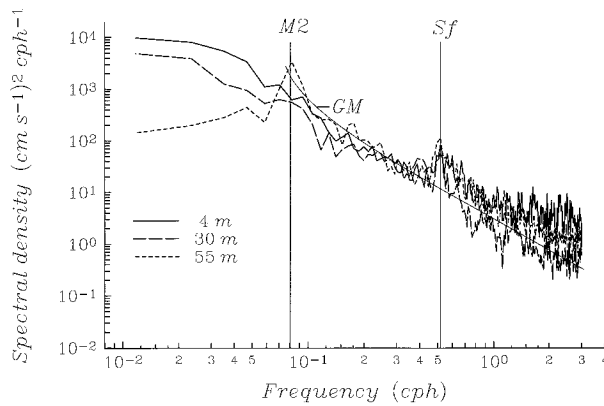


FIG. 7. Energy density spectra of current records from Gullmar Fjord in August 1974 and the model spectrum GM.

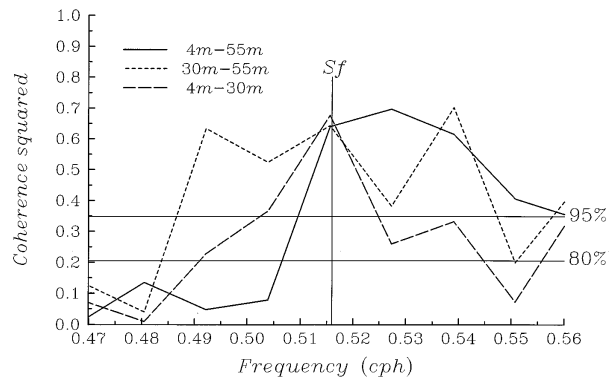


FIG. 8. Squared coherence with significance levels for the seiche frequency band.

difference between the two layers that is a factor of 1.5 greater than the value used for the model computations.

The description of the density field in the fjord is based upon monthly profiles. This is admittedly very sparse since it is known that quite rapid changes of the density field may occur in the Skagerrak (e.g., Gustafsson and Stigebrandt 1996) and, as consequence of this, in Gullmar Fjord (Djurfeldt 1987). Thus, there is a substantial uncertainty with regard to the density field, which may explain some of the difference between observed and computed damping of the seiche. We have also made the approximation that the internal waves generated at the Skagerrak side of the sill obtain the same energy transfer from the seiche as the waves generated inside the fjord. These uncertainties may contribute an additional explanation for the discrepancy between theory and observations.

We have also analyzed current meter records obtained in August 1974 for quite different purposes (cf. section 4). Unfortunately there is no simultaneous sea level record so one cannot relate the recorded currents to an actual seiche event. The location of the current meter rig on the slope of the sill (Fig. 1), where small-scale topographical features may also influence the recorded currents, is not perfect for observing internal waves radiating away from the wave generator (the fjord sill). For this one would have preferred current measurements well away from the wave generator. However, we believe that it is still of interest to show that the currents at seiche frequency have strong baroclinic components that are hard to explain by mechanisms other than internal wave generation at the sill.

Applying spectral analysis to the time series of the current meter data, energy density spectra are obtained from each current meter. The coherence and phase between the current meters are calculated. Here, 16 degrees of freedom have been used from 4096 points to obtain good significance of the coherence; see Thompson (1979). The seiche frequency S_f is estimated to be 0.516 cph, that is, a period of $T = 116$ min. (Fig. 7).

This frequency has high energy density in all records and there is high coherence between the current meters (Fig. 8). There is much energy in a bandwidth of about ± 0.078 cph around this frequency, indicating that the period T of the seiche may vary in the interval $100 < T < 140$ min. To obtain the mean current amplitude it is necessary to integrate over the bandwidth. Such an integration gives mean speeds of 1.5 cm s^{-1} (at 4 m), 1.2 cm s^{-1} (at 30 m), and 1.7 cm s^{-1} (at 55 m). As already mentioned there is no sea level record for the period of the current measurements. Accounting for the probability of occurrence of the seiche in August ($P \approx 0.4$, see Fig. 3) speeds are estimated to be in the range $3\text{--}4 \text{ cm s}^{-1}$.

Seiching events apparently occur occasionally and the amplitude of the seiche in each event declines quite rapidly. In addition, the seiche frequency is variable. Spectral and harmonic analyses are thus not perfect methods to analyze seiches. However, to demonstrate the character of the currents we show results from the spectral analysis for the frequency $\omega = 9.0 \times 10^{-4} \text{ s}^{-1}$ for which the results are statistically highly significant. The current at 55 m lags the current at 30 m by 166 deg and the current at 4 m leads the current at 30 m by 92 deg. This clearly shows that more than one baroclinic component is present. Since we have neither independent information about the barotropic mode (no sea level record for this period) nor the vertical stratification for the whole period, we may only conclude that the current measurements show strong baroclinic components.

The dominating semidiurnal tidal constituent M_2 , is also marked in Fig. 7. Above the sill, at depths 4 and 30 m there is no accentuated semidiurnal peak and the low-frequency part of the spectra (sub-semidiurnal) looks much like spectra usually obtained at nearby offshore locations (cf. Shaffer and Djurfeldt 1983). However, the transmittance of low-frequency subinertial motions from the coastal water to the basin water, below the fjord sill, is obviously weak, probably due to the shielding effect of the sill in combination with stable stratification in the basin water. This enhances the ap-

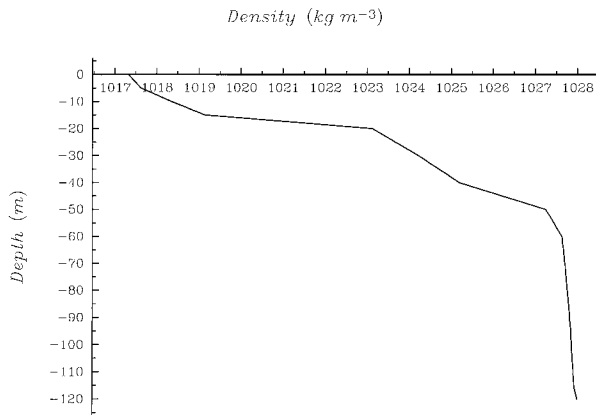


FIG. 9. Observed density stratification in the fjord 28 August 1974.

pearance of the semidiurnal energy peak at 55 m, which may be explained as due to internal tidal waves generated at the sill. Unfortunately, the coherence for this frequency is weak, wherefore the vertical variation of the phase is uncertain. One exception is for the phase difference between 30 and 55 m, which is about 85 deg with a squared coherence of 0.36 (about 95% significance). This result is also confirmed by harmonic analysis, which gives a corresponding phase difference of 95 deg.

In Fig. 7 we have also included for comparison the modal energy spectrum GM from Garrett and Munk (1972, 1975). This spectrum is assumed to describe the energy level in the internal wave field in the ocean. The GM spectrum is given by

$$F_u(\omega) = 4\pi E b^2 N_0 N f \frac{\omega^2 + f^2}{\omega^3 \sqrt{\omega^2 - f^2}}, \quad (17)$$

where the empirical parameters $E = 6.3 \times 10^{-5}$, $b = 1.3$ km, and $N_0 = 5.2 \times 10^{-3} \text{ s}^{-1}$ are the nondimensional energy level, the vertical buoyancy scale depth, and the buoyancy frequency respectively. The latter is assumed to have an exponential profile given by

$$N(z) = N_0 e^{-z/b}. \quad (18)$$

For this particular fjord, the inertial frequency f is about $1.24 \times 10^{-4} \text{ s}^{-1}$ and the buoyancy frequency N , obtained from the density profile in Fig. 9, is about 2.41×10^{-2} , 3.17×10^{-2} , and $1.83 \times 10^{-2} \text{ s}^{-1}$ at 4, 30, and 55 m respectively. We have used the mean buoyancy frequency (2.47×10^{-2}).

The spectra from the current meters are more energetic than the modal GM spectrum (Fig. 7) for the seiche frequency and higher frequencies, indicating that there is an energy input at the seiche frequency.

6. Concluding remarks

A model for the damping of a barotropic seiche through baroclinic wave drag has been applied to the

Gullmar Fjord. According to the model, about 1% of the initial seiche energy remains after 8.5 h for typical stratification, which corresponds well with the observed damping. The model predicts that the damping of seiches varies with the density stratification, as verified by the observed damping. Ordinary bottom friction can explain at most 1% of the observed damping in the fjord. Therefore, bottom friction may be neglected as a mechanism for seiche damping in this fjord, and probably also in other deep fjords. Furthermore, from the rapid generation of seiches it seems that the forcing of seiches does not influence the decay process.

Analysis of the 1985 sea level record shows that the seiche period T is in the interval $90 < T < 132$ min and the mean period is 1 h 55 min. There are seasonal variations in the seiche amplitude a_i , and in the probability of occurrence P , probably reflecting the activity of seiche generating mechanisms. The annual mean values are $a_i = 4.4$ cm and $P = 0.33$.

Spectral analysis was applied to current meter data from the fjord-side slope of the sill for August 1974. Three current meter records were analyzed, and from coherence and significance levels the seiche frequency is estimated to be 0.516 cph, that is, 116 min. However, there is much energy in a band around this frequency indicating that the period of the seiche may vary in the interval $100 < T < 140$ min, a result in accordance with that from the sea level record analysis. The vertical variation of the current phase indicates that the motion has strong baroclinic components. This result further strengthens the conclusion that the damping of the seiche is due to baroclinic wave drag.

Equation (13) shows that the coefficient of damping due to baroclinic wave drag is proportional to ω^2 . Higher seiche modes are therefore much more strongly damped than the fundamental mode. The second mode should have a damping coefficient 9 times greater than the first (fundamental) mode. Baroclinic wave drag should thus act as an efficient low-pass filter on the barotropic natural modes of oscillation, which may be the reason why the fundamental mode is so dominating in Gullmar Fjord.

In most sill fjords the tides are the dominating energy source for mixing processes. Stigebrandt and Aure (1989) observed that about 5% of the energy transferred from the surface tide to internal tides at sills is used for mixing in the basin water of most fjords. Internal waves generated at the sill by a barotropic seiche should also contribute energy to mixing processes. In Gullmar Fjord the mean energy flux by such internal waves when occurring is about 145% of the mean energy flux by internal tidal waves. Here the annual mean values of the squared observed amplitudes have been used, which are about 23 cm² for the seiche and about 273 cm² for the tide. The annual mean value of the squared angular frequency of the seiche is $8.4 \times 10^{-7} \text{ s}^{-2}$. For the annual timescale, for which $P = 0.33$, we find that the energy transfer to internal waves generated by the seiche should

be about 48% of the energy transfer from the tides to internal tidal waves. Thus, the energy transfer from seiches to internal waves and turbulent mixing processes in the basin water should be quite significant in Gullmar Fjord. This makes it particularly interesting to find out how the seiche is generated.

It is interesting to note that the fjord sill in combination with stable vertical stratification effectively hinder motions of periods longer than semidiurnal from penetrating into the basin of the fjord, as recorded by the current meter at 55-m depth. However, for periods shorter than semidiurnal the velocity spectrum in the basin is very similar to those above the sill level.

Finally, it may be noted that seiching seems to be much more common in inland lakes than in fjords. The major reason for this may be that seiche damping by baroclinic wave drag in general is much more efficient in fjords where the nodal line (with maximum transport) is at the mouth. In lakes, however, the nodal line is situated about midway between the ends of the lake where often the cross-sectional area is maximal and the bottom topography smooth.

Acknowledgments. The authors are grateful to SMHI for the opportunity to use their hydrographic database. The current meter data were placed at our disposal by Dr. Lars Rydberg. This work was supported by the Swedish Natural Science Research Council (NFR).

REFERENCES

- Baines, P. G., 1982: On internal tide generation models. *Deep-Sea Res.*, **29**, 307–338.
- de Young, B., and S. Pond, 1989: Partition of energy loss from the barotropic tide in fjords. *J. Phys. Oceanogr.*, **19**, 246–252.
- Djurfeldt, L., 1987: On the response of the fjord Gullmaren under ice cover. *J. Geophys. Res.*, **92**, 5157–5167.
- Garrett, C., and W. H. Munk, 1972: Space-time scales of internal waves. *Geophys. Fluid Dyn.*, **2**, 225–264.
- , and —, 1975: Space-time scales of internal waves. A progress report. *J. Geophys. Res.*, **80**, 291–297.
- Gill, A. E., 1982: *Atmosphere Ocean Dynamics*. Academic Press, 662 pp.
- Gustafsson, B., and A. Stigebrandt, 1996: Dynamics of the freshwater-influenced surface layers in the Skagerrak. *Neth. J. Sea Res.*, **35**, 39–53.
- Kullenberg, B., 1932: A recording boundary gauge for the open sea. *Göteborgs Vetensk-Vitterhets-Samh. Handl. Ser. B*, **9**, 1–9.
- Pettersson, H., 1917: Stående vågor i havet. *Medd. Geogr. Föreningen i Göteborg 1917*, **2**, 29–44.
- , 1921: Meteorological influences on the level of the sea-surface. *Geogr. Annaler 1921*, **H. 1–2**, 165–182.
- Proudman, J., 1953: *Dynamical Oceanography*. Methuen, 409 pp.
- Rattray, M., 1960: On the coastal generation of internal tides. *Tellus*, **12**, 54–62.
- Shaffer, G., and L. Djurfeldt, 1983: On the low frequency fluctuations in Skagerrak and Gullmaren. *J. Phys. Oceanogr.*, **13**, 1321–1340.
- Sjöberg, B., and A. Stigebrandt, 1992: Computations of the geographical distribution of the energy flux to mixing processes via internal tides and the associated vertical circulation in the ocean. *Deep-Sea Res.*, **39**, 269–291.
- Stigebrandt, A., 1976: Vertical diffusion driven by internal waves in a sill fjord. *J. Phys. Oceanogr.*, **6**, 486–495.
- , 1980: Some aspects of tidal interaction with fjord constrictions. *Estuar. Coastal Mar. Sci.*, **11**, 151–166.
- , and J. Aure, 1989: On vertical mixing in basin waters of fjords. *J. Phys. Oceanogr.*, **19**, 917–926.
- Svansson, A., 1984: Hydrography of the Gullmar Fjord. *Medd. Havsfiskelaboratoriet, Lysekil.*, **297**, 1–21.
- Thompson, R. O. R. Y., 1979: Coherence significance levels. *J. Atmos. Sci.*, **36**, 2020–2021.
- Zeilon, N., 1912: On the tidal boundary waves and related hydrodynamical problems. *Kungl. Svenska Vetenskapsakademiens Handlingar*, Vol. **47** (4), 46 pp.
- , 1913: On the seiches of the Gullmar Fjord. *Sven. Hydrogr. Biol. Komm. Skr.*, **V**, 1–17.